Remote Sensing of Environment 132 (2013) 120–130

Contents lists available at SciVerse ScienceDirect

Remote Sensing of Environment

journal homepage: www.elsevier.com/locate/rse

Effect of image spatial and spectral characteristics on mapping semi-arid rangeland vegetation using multiple endmember spectral mixture analysis (MESMA)

K.R. Thorp [a,*], A.N. French [a], A. Rango [b]

[a] USDA-ARS, U.S. Arid Land Agricultural Research Center, 21881 N Cardon Ln, Maricopa, AZ 85138, United States
[b] USDA-ARS, Jornada Experimental Range, P.O. Box 30003, MSC 3JER, NMSU, Las Cruces, NM 88003, United States

ARTICLE INFO

Article history:
Received 19 September 2012
Received in revised form 20 November 2012
Accepted 9 January 2013
Available online xxxx

Keywords:
AVIRIS
CAI
Creosote
Grass
Hyperspectral
HyspIRI
Imaging spectroscopy
Mesquite
NDVI
Nonphotosynthetic
Spatial scale
Spectra

ABSTRACT

Encroachment of invasive shrubs into grassland areas on rangelands in the southwestern United States threatens the viability of livestock production and can severely alter hydrology and biodiversity. Novel remote sensing technologies may provide useful information for monitoring and remediating this threat. The objectives were to investigate multiple endmember spectral mixture analysis (MESMA) as an approach to map rangeland vegetation using hyperspectral remote sensing imagery and to test the sensitivity of MESMA to alternative image spatial resolutions and spectral waveband combinations. Data from two Airborne Visible/Infrared Imaging Spectrometer (AVIRIS) overflights at the Jornada Experimental Range in southwestern New Mexico were used in the analysis. Endmember spectra were selected from a library of ground-based spectral observations collected with a field spectroradiometer. A 4-endmember MESMA was conducted for both AVIRIS images at their native spatial resolutions using 113 10-nm wavebands from 422 to 2339 nm. Additional MESMAs were conducted at 10 multiples of the images' native spatial resolution and for 6 alternative combinations of spectral waveband subregions. Maps of endmember fractional cover for green shrub vegetation, nonphotosynthetic grass vegetation, and bare soil were comparable to an earlier vegetation classification map of Jornada. MESMA fractional cover estimates for the green vegetation endmember were positively correlated with the normalized difference vegetation index (NDVI) with correlation coefficients (r) greater than 0.58. Correlation coefficients between the sum of the green and nonphotosynthetic vegetation endmembers and the cellulose absorption index (CAI) were greater than 0.59. Correlation coefficients between MESMA fractional green vegetation cover and NDVI from independent multispectral images were greater than 0.57. Despite losses in spatial detail at coarser image spatial resolutions, MESMA results for images with spatial resolution degraded by a factor of 10 (~150 m) were similar to aggregated results for MESMA at the native spatial resolution (~15 m). Additionally, MESMA results were shown to be substantially more sensitive to the spectral wavebands used in the analysis as compared to the spatial resolution of the images. Considered together, the MESMA results at Jornada indicated that fine spectral resolution with hyperspectral remote sensing was substantially more important than incremental changes in image spatial scale from 15 m to 150 m.

Published by Elsevier Inc.

1. Introduction

Over the past century, rangelands in the northern Chihuahuan Desert have been severely degraded due to livestock overgrazing and other human activities (Hoyt, 2002). Drought and climate change have also played a role (Chehbouni et al., 2000). Several focused studies of vegetation change at the Jornada Experimental Range (Jornada) in southwestern New Mexico have documented the encroachment of invasive shrubs, such as mesquite (*Prosopis glandulosa*), creosote bush (*Larrea tridentata*), and tarbush (*Flourensia cernua*), into areas once dominated by grass. These intrusions have led to severe losses in grassland vegetation at Jornada (Buffington and Herbel, 1965; Gibbens et al., 2005). Unsuccessful efforts to remediate grasslands by shrub removal suggest that shrub invasion leads to soil erosion and hydrologic alterations, which impede the reestablishment of grass species (Rango et al., 2005).

Continued efforts to monitor and remediate these threats to rangeland environments will be bolstered by the availability of remote sensing technologies and the development of novel remote sensing instrumentation and data processing algorithms. Previous approaches using aerial photography at Jornada have been narrowly focused and lacking in spectral information (Rango et al., 2005). Comprehensive, rapid, and repeated viewing of large rangeland areas will require deployment of sensors at high altitude or from orbit. With the advent of airborne hyperspectral remote sensing instrumentation such as AVIRIS (Green et al., 1998), analyses using hyperspectral data to characterize rangeland degradation and monitor vegetation change are increasing (Asner and Heidebrecht, 2002; Asner et al., 2000; Li et al., 2005; Mansour et al., 2012; Yang et al., 2009). Further investigation of

* Corresponding author. Tel.: +1 520 316 6375; fax: +1 520 316 6330.
E-mail address: kelly.thorp@ars.usda.gov (K.R. Thorp).

0034-4257/$ – see front matter. Published by Elsevier Inc.
http://dx.doi.org/10.1016/j.rse.2013.01.008

these novel remote sensing techniques is required before the technology can deliver on its promise to guide policy development and support long-range planning for better management of rangelands.

The primary advantage of hyperspectral remote sensing over current multispectral techniques is its ability to resolve the reflectance responses of image features with fine spectral detail, usually in hundreds of narrow, contiguous spectral wavebands. Hyperspectral observations of homogeneous vegetation canopies may demonstrate unique responses over certain waveband regions as compared to that for other plant species or soil backgrounds (Thenkabail et al., 2000). In cases where vegetation canopies are not homogeneous or where spatial resolution is too coarse to avoid mixed pixels, spectral mixture analysis can be used to resolve fine scale land surface features. Spectral mixture analysis (SMA) is a hyperspectral data processing approach that quantifies the proportions of land surface features within mixed pixels using knowledge of each feature's pure spectral response or "endmember."

A major limitation of SMA is that every image pixel is unmixed using the same endmember spectra. This is problematic when a feature is present only in certain portions of the image or when a feature exhibits substantial spectral variation that is not well represented by one endmember spectral observation (Dennison and Roberts, 2003). Multiple endmember spectral mixture analysis (MESMA) addresses these problems by testing multiple combinations of endmembers and endmember spectra for each pixel in the image (Roberts et al., 1998). Thus, MESMA increases the flexibility of simple SMA. As compared to common multispectral approaches, the main advantage of SMA and MESMA is their ability to facilitate remote sensing data analyses using full spectrum information.

Image spatial and spectral resolutions are expected to influence MESMA outcomes. However, the sensitivity of MESMA results to these factors has not been quantified. A better understanding of MESMA performance constraints is informative for the development of novel hyperspectral imaging systems. For example, the National Aeronautics and Space Administration (NASA) is currently developing the Hyperspectral Infrared Imager (HyspIRI) and is planning for the instrument's deployment by satellite (hyspiri.jpl.nasa.gov). HyspIRI will include an imaging spectrometer observing from 380 nm to 2500 nm in 10 nm contiguous bands and a multispectral imager observing from 3 to 12 μm. These instruments will provide images with spatial resolution of 60 m at a nadir view angle. Given these design characteristics, images from other sensors can be used to simulate and evaluate HyspIRI data sets prior to launch. Images from the AVIRIS sensor are useful for evaluations of the HyspIRI imaging spectrometer, because AVIRIS spectral resolution is similar to HyspIRI (aviris.jpl.nasa.gov). Also, the spatial resolution of the AVIRIS sensor, flown at the typical altitude of 20 km, is 4 times finer than that proposed for HyspIRI, which allows for assessments of the effects of HyspIRI's coarser spatial resolution on data analysis.

The first objective was to investigate multiple endmember spectral mixture analysis (MESMA) as an approach to map rangeland vegetation using hyperspectral remote sensing data, such as that currently obtained with AVIRIS and proposed for HyspIRI. The Jornada Experimental Range was the field site used for the analysis. The second objective was to test the sensitivity of MESMA results to degradations in image spatial resolution and to the use of alternative spectral wavebands. The latter objective supports design efforts for the HyspIRI sensor prior to launch.

2. Materials and Methods

2.1. Jornada Experimental Range

The Jornada Experimental Range (Jornada; jornada.nmsu.edu) was established by the United States Department of Agriculture in 1912 to develop effective strategies for management of livestock grazing lands. It is a 783 km^2 semiarid rangeland located on the Jornada del Muerto Plain in the northern part of the Chihuahuan Desert in southwestern New Mexico, roughly 37 km northeast of the city of Las Cruces and 40 km west of the White Sands National Monument (Fig. 1). Similar to the analysis of Jornada vegetation provided by Gibbens et al. (2005), the analysis reported herein focuses on the 582 km^2 Jornada plain west of the San Andres Mountains. Jornada has been a National Science Foundation Long-Term Ecological Research site since 1981. Havstad et al. (2000) provide a detailed description of Jornada and its historical use as a site for evaluation of satellite remote sensing systems, including the JORNEX and PROVE (Privette et al., 2000) experiments.

2.2. Airborne Imaging Spectroscopy

The AVIRIS imaging spectrometer (Green et al., 1998) was used to collect remote sensing images over Jornada on several dates from 1997 to 2002. The present analysis focused on two of those dates: June 15, 2001 and October 9, 2002. The instrument was deployed using an airborne platform flying approximately 20 km above sea level. AVIRIS collected radiometric observations between 380 nm and 2500 nm using 224 unique detectors each with a nominal spectral bandwidth of 10 nm. A whiskbroom scanning mirror with a 12 Hz scanning rate was used to obtain cross-track spatial samples.

Five flight lines were required to obtain full coverage of Jornada on each acquisition date. Preliminary data processing steps, including geometric and radiometric correction, were completed by the AVIRIS Data Facility. Images were georeferenced using a geometric look-up table constructed using data from the navigation equipment aboard the aircraft. Images were also calibrated to spectral radiance.

Further data preprocessing, including atmospheric correction and additional georeferencing, was conducted in-house. Atmospheric correction was accomplished with the Second Simulation of a Satellite Signal in the Solar Spectrum (6S) algorithm (Kotchenova et al., 2006). Based on the cross-track spatial sampling interval of 0.87 milliradians, the viewer zenith angle was calculated at intervals of 25 pixels across the image swath, and 6S parameters for the remaining pixels were interpolated. Since all images were collected along a due north or due south flight line, viewer azimuth angles were set at 90° and 270° for pixels east and west of the flight line, respectively. Solar zenith and azimuth angles were computed at the time and position of the aircraft midway through the data acquisition period for each image (Reda and Andreas, 2004). Atmospheric profiles for pressure, temperature, and water density from ground-level to the sensor-level were obtained from the National Center for Environmental Prediction (NCEP) Reanalysis data set, provided by the NOAA/OAR/ESRL PSD, Boulder, Colorado, USA (http://www.esrl.noaa.gov/psd/). The data set contains long-term, high-resolution climate information for the North American domain (Mesinger et al., 2006). The NCEP data nearest in time and space to the AVIRIS overflights at Jornada were used to specify the 6S parameters for atmospheric profile. The 6S default "Desert Model" with a visibility of 16 km was used to define the aerosol profile. Spectral conditions were assumed to be monochromatic; 6S was provided the wavelength at the center of each of AVIRIS waveband. Lambertian ground reflectance was assumed. Given the complexity of correcting multiple bands and scenes, a Python script (www.python.org) was developed to conduct 6S simulations and atmospherically correct the AVIRIS images.

Automated methods at the AVIRIS Data Facility provided major help with image geometric corrections. However, additional corrections were needed to properly mosaick the five images on each data collection date. Images were therefore corrected further by selecting ground control points from an orthophoto provided by the United States Geological Survey (USGS). Approximately 50 points per image were required for improving the image registration. Images were then georegistered using polynominal warping

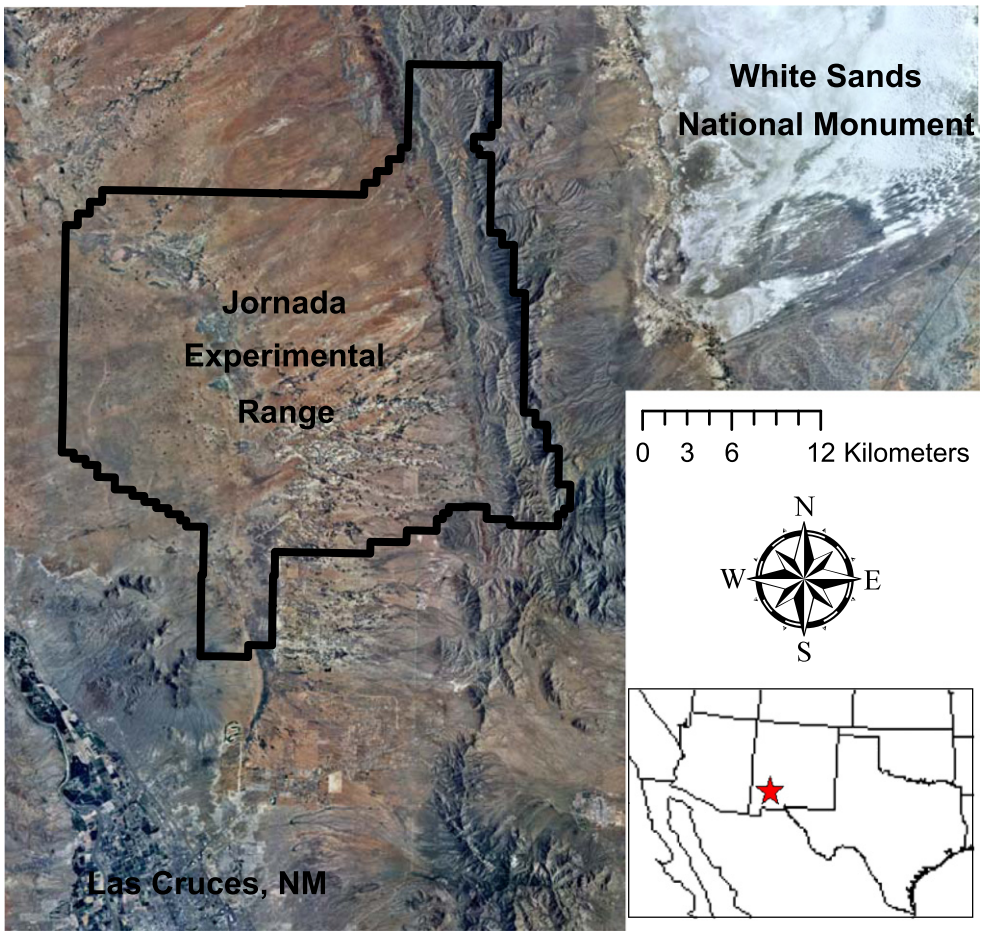

Fig. 1. Site map for the Jornada Experimental Range in southwestern New Mexico, USA. Orthophoto data were obtained from the U.S. Geological Survey (earthexplorer.usgs.gov).

with nearest neighbor resampling. To prepare for mosaicking the images were resampled to the average spatial resolution of the original images: 16.6 m for the 2001 images and 15.5 m for the 2002 images. This best preserved the spatial resolution of the original images. The five images from each data collection date were then mosaicked, and the mosaicked images were clipped to the boundaries of Jornada. These tasks were completed using the Environment for Visualizing Images (ENVI) software (Version 4.8, Exelis Visual Information Solutions, Boulder, CO).

2.3. Endmember Spectra

Endmember spectra for conducting MESMA on the AVIRIS images were selected from ground-based observations of rangeland vegetation using a portable field spectroradiometer (FieldSpec Pro, Analytical Spectral Devices, Inc., Boulder, CO). Radiometric measurements were collected in 2151 narrow wavebands from 350 to 2500 nm with a bandwidth of 1 nm. The instrument was equipped with a 25° field-of-view fiber optic cable, which was positioned approximately 1.5 m above the ground. Spectral measurements typically occurred around the time of solar noon. Frequent radiometric observations of a calibrated, 99% Spectralon panel (Labsphere, Inc., North Sutton, New Hampshire) were used to characterize solar irradiance throughout the data collection period. Canopy reflectance factors in each waveband were computed as the ratio of the canopy radiance over the corresponding time-interpolated value for solar irradiance.

Ground-based radiometric measurements were collected on May 5 and May 8 in 2001, approximately six weeks prior to the AVIRIS overflight on June 15. In 2002, ground-based observations were collected on October 4, five days prior to the AVIRIS overflight on October 9. Radiometric measurements were collected along predefined transects at locations dominated by mesquite, grass, creosote bush and tarbush. A fifth transect was located in an area that was transitioning from grass to mesquite. Between 125 and 200 scans were collected at regular intervals (every few meters) along each transect. The features within the sensor's field-of-view were documented for each scan. The authors credit Dr. Jerry Ritchie (1937–2009), former Research Soil Scientist at USDA-ARS and long-term contributor at Jornada, for his efforts to collect and organize these spectral data sets.

To select endmembers for MESMA, spectral scans that were documented as a mixture of bare soil and vegetation were eliminated, because MESMA requires “pure” spectra for each feature class. Remaining scans were separated into five classes, including mesquite, creosote bush, tarbush, grass, and bare soil. These scans were assessed graphically by plotting the data and numerically by calculating the well-known normalized difference vegetation index (NDVI) and plotting histograms of this index. These inspections were useful for finding and eliminating erroneous entries. Further culling of endmember spectra was accomplished with MESMA techniques. A Python program handled the adjustment of the spectrometer data to match the AVIRIS wavebands.

2.4. Multiple Endmember Spectral Mixture Analysis (MESMA)

An open-source plug-in for the ENVI software called Visualization and Image Processing for Environmental Research (VIPER) Tools (Version 1.5, www.vipertools.org) was used to implement MESMA for these data sets. The tool facilitates the creation and management of endmember spectral libraries, the statistical analysis of separability among spectral classes, and the implementation of MESMA algorithms. MESMA based on one, two, or three unique spectral libraries

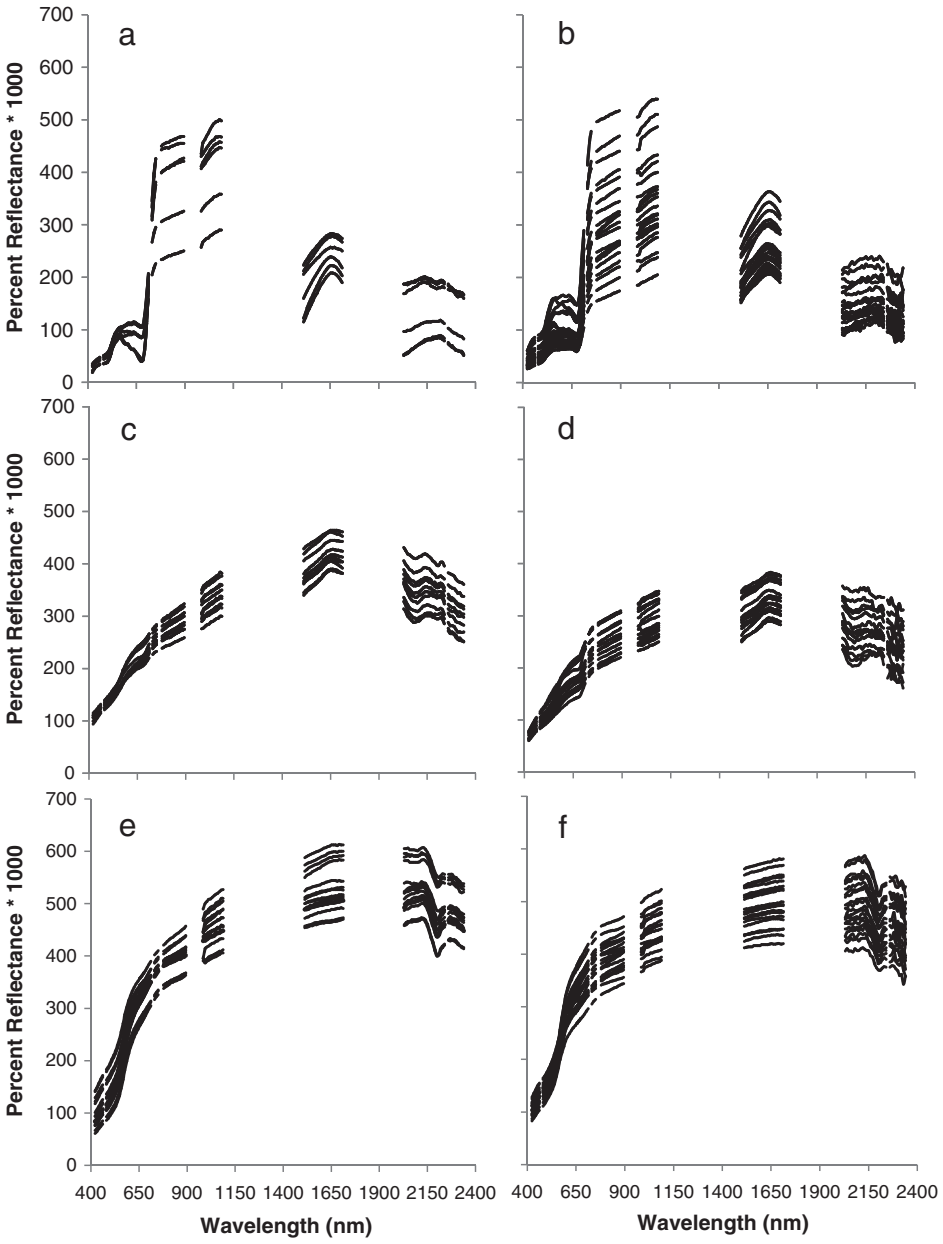

Fig. 2. Endmember spectra used for multiple endmember spectral mixture analysis (MESMA) of AVIRIS images at the Jornada Experimental Range. Spectra of green shrub vegetation in a) May 2001 and b) October 2002, nonphotosynthetic grass vegetation in c) May 2001 and d) October 2002, and bare soil in e) May 2001 and f) October 2002 were collected with a field spectroradiometer.

can be conducted. Each spectral library represents one endmember, but can contain multiple spectra. MESMA then "unmixes" each pixel in the image by testing all possible combinations of spectra included in these spectral libraries. Final endmember fractions are assigned to each pixel based on the endmember combination that gives the lowest root mean squared error (RMSE) between modeled and observed spectral responses. Each MESMA includes an additional endmember for shade, which can be either provided by the user or defaulted to zero (photometric shade). The latter option was used for all analyses in this study. The minimum allowable endmember fraction, maximum allowable endmember fraction, and maximum allowable shade fraction were set to values of −0.05, 1.05, and 0.8, respectively. By allowing endmember fractions slightly greater than 1.00 and slightly less than 0.00, MESMA was permitted to consider models that fit well in spite of endmember fractions that were slightly physically unrealistic. Otherwise, these potentially worthwhile models would have been eliminated from consideration. No RMSE or residual constraints were used for MESMAs in this study.

Five unique spectral libraries, one for each of the five feature classes, were created with the scans from the ground-based spectroradiometer in each year. Due to possible seasonal variation in vegetation phenology, the ground-based spectral data from the two years were handled separately. Five two-endmember MESMAs were then conducted on each AVIRIS image as an approach to identify the scans from each class that were best able to unmix the image. Following these analyses, only the endmember spectra that were able to classify greater than 0.1% of the total image area were retained. This procedure reduced the number of possible endmember combinations and thus reduced the computational time required for subsequent four-endmember MESMA.

Endmember spectra remaining after the two-endmember analysis were tested for spectral separability among classes using the VIPER Tools "square array" computation, which reports several statistical

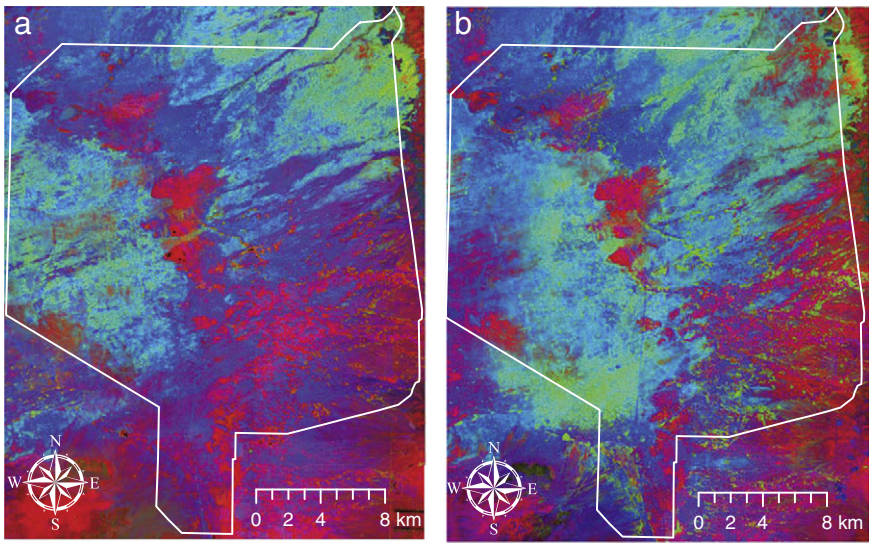

Fig. 3. Multiple endmember spectral mixture analysis (MESMA) result for a) June 15, 2001 AVIRIS imagery and b) October 9, 2002 AVIRIS imagery over the Jornada Experimental Range. Results are displayed as an RGB image where R, G, and B represent fractional cover of nonphotosynthetic grass, green shrub vegetation, and bare soil, respectively.

metrics on the use of each spectrum to unmix each of the other spectra in a spectral library. From the square array data, the average RMSE for each spectrum to model other spectra within each of the five classes was calculated. If an endmember spectrum was better at modeling spectra outside its own class than within it, the spectrum was visually inspected and considered for elimination from the analysis.

After these efforts to fine tune the endmember spectra, the remaining endmembers were incorporated into three spectral libraries representing green vegetation (shrubs), nonphotosynthetic vegetation (grass), and bare soil for each year (Fig. 2). The NDVI for mesquite, tarbush, and creosote bush spectra was not less than 0.42, so these spectra were merged to represent a green vegetation endmember class. The NDVI for grass spectra did not exceed 0.16, so grass spectra were incorporated into an endmember class for nonphotosynthetic vegetation. A third endmember class was established for bare soil. Using these three endmember classes plus a fourth for shade, a four-endmember MESMA was conducted for the AVIRIS images in each year.

2.5. Waveband Elimination

Preliminary analyses demonstrated the sensitivity of MESMA results to the spectral wavebands included, and several issues necessitated that some wavebands be removed from the analysis. For example, wavebands falling outside the optimal ranges of the three detectors in the ground-based spectroradiometer were usually characterized by a low signal-to-noise ratio. Also, due to limited input data, the 6S atmospheric corrections of the AVIRIS data were unreasonable for some wavebands, particularly those at atmospheric absorption bands. Several graphical and quantitative approaches were used to identify the wavebands that needed to be removed from the analysis. These procedures eliminated nearly half of the wavebands from the data sets, so that MESMA was conducted using only 113 of the original 224 wavebands. These 113 bands were located mainly within the visible and NIR region from 422 to 1088 nm (VIS/NIR) and within the SWIR region from 1513 to 1712 nm (SWIR1) and from 2030 to 2339 nm (SWIR2) (Fig. 2).

Table 1
Evaluation of 2001 and 2002 MESMA endmember fractional cover results at Jornada.[a]

	Bias[b]	r[c]	2001 NDVI[d]	2001 CAI[e]	2002 NDVI[f]	2002 CAI[g]	SW NDVI[h]	NW NDVI[i]
EM1 GV	−0.08	0.41	0.73	−0.20	0.58	0.02	0.71	0.57
EM2 NPV	0.10	0.66	−0.59	0.56	−0.25	0.40	−0.61	−0.71
EM3 Soil	0.11	0.67	−0.01	−0.89	−0.35	−0.79	0.35	0.41
EM4 Shade	−0.13	0.39	0.20	0.41	0.07	0.09	−0.22	−0.18
EM1 + EM2	0.02	0.55	−0.11	0.59	0.25	0.60	−0.22	−0.23

[a] Multiple endmember spectral mixture analysis (MESMA); southwest (SW); northwest (NW); normalized difference vegetation index (NDVI); cellulose absorption index (CAI); endmember (EM); green vegetation (GV); nonphotosynthetic vegetation (NPV).
[b] Average fractional cover bias between 2001 and 2002 MESMA results.
[c] Pearson correlation between 2001 and 2002 MESMA results.
[d] Pearson correlation between 2001 MESMA result and 2001 AVIRIS NDVI.
[e] Pearson correlation between 2001 MESMA result and 2001 AVIRIS CAI.
[f] Pearson correlation between 2002 MESMA result and 2002 AVIRIS NDVI.
[g] Pearson correlation between 2002 MESMA result and 2002 AVIRIS CAI.
[h] Pearson correlation between 2001 MESMA result and 2001 SW IKONOS NDVI.
[i] Pearson correlation between 2001 MESMA result and 2001 NW IKONOS NDVI.

2.6. MESMA Evaluation

Remote sensing is attractive for rangeland monitoring, because it can rapidly and comprehensively map large land areas using a small fraction of the time and labor needed for ground-based reconnaissance. The irony is the difficulty in evaluating the results of remote sensing data analyses, because comprehensive ground-based data sets for this purpose are typically prohibited by the cost and labor required to collected them. For the case of Jornada, intensive ground reconnaissance in 1998 and a set of aerial photographs collected in 1996 were used by (Gibbens et al., 2005) to construct maps that delineated the location of dominant vegetation types across Jornada. However, fractional vegetation cover was not quantified in these maps, and the vegetation cover delineations were not resolved to 15 m spatial resolution. Thus, while the historical maps provided essential context for land cover delineation at Jornada, they were insufficient for validation of the MESMA results derived from AVIRIS. As an alternative, three approaches were adopted to ensure quantitative consistency and reasonableness: 1) comparing the MESMA results for 2001 with that for 2002, 2) comparing the MESMA results with known spectral indices, and 3) comparing the 2001 MESMA results with an analysis of two IKONOS images at 4 m spatial resolution collected over a subsection of Jornada on May 23, 2001.

2.6.1. MESMA Annual Comparison

Efforts to preserve the original spatial resolution of the AVIRIS data resulted in MESMA images with slightly different spatial scales: 16.6 m for the 2001 images and 15.5 m for the 2002 images.

Therefore, results could not be directly compared, pixel by pixel. Instead, a set of 10,000 points was randomly generated within the Jornada boundary and the MESMA results for 2001 and 2002 were sampled at these locations. MESMA endmembers were assessed by calculating the average bias, Pearson's correlation coefficient, and Spearman's rank correlation coefficient between the results for the two years.

2.6.2. MESMA and spectral indices

Pearson's correlation coefficients were calculated between the fractional cover of each MESMA endmember and two spectral indices, including the well-known normalized difference vegetation index (NDVI) and the cellulose absorption index (CAI) developed by Nagler et al. (2003). The NDVI (Rouse et al., 1973) was calculated as

$$\mathrm{NDVI} = \frac{R_{\mathrm{NIR}} - R_{\mathrm{RED}}}{R_{\mathrm{NIR}} + R_{\mathrm{RED}}} \quad (1)$$

where R_{NIR} is the spectral reflectance in the near-infrared region and R_{RED} is the spectral reflectance in the red region. Based on the third and fourth Landsat TM bands, the AVIRIS data in 9 bands from 635 to 683 nm and in 13 bands from 779 to 894 nm were averaged to estimate the red and NIR waveband reflectances, respectively. Focused in the SWIR2 region, the CAI was calculated as

$$\mathrm{CAI} = 100.0 * \left[\frac{R_{2030} + R_{2210}}{2.0} - R_{2100}\right] \quad (2)$$

where R_{2030}, R_{2210}, and R_{2100} are narrow-band reflectances at 2030, 2210, and 2100 nm, respectively. The AVIRIS reflectances in the waveband nearest to these required wavelengths were used to calculate CAI. The CAI is commonly used to estimate crop residue or plant litter cover. Positive CAI values indicate the presence of cellulose, and values can reach 6.0 for full crop residue cover (Nagler et al., 2003).

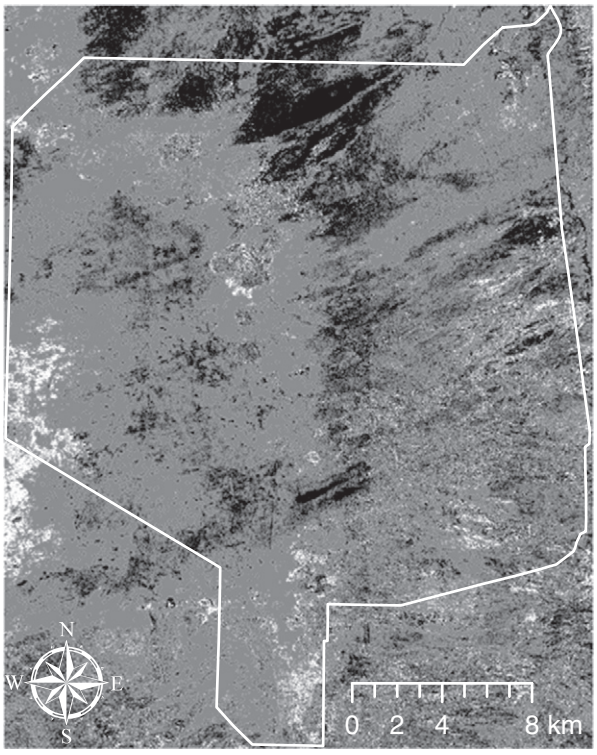

Fig. 4. Classification map of creosote bush (black), mesquite (grey), and tarbush (white) species based on multiple endmember spectral mixture analysis (MESMA) of an October 9, 2002 AVIRIS image over the Jornada Experimental Range.

2.6.3. MESMA and IKONOS Images

Two IKONOS images (GeoEye, Herdon, VA) were collected over Jornada on May 23, 2001, which was 23 days prior to the AVIRIS overflight in that year. Each image covered approximately 118 km^2, one focusing on the northwestern portion of Jornada and the other focusing on the southwestern portion. The multispectral IKONOS sensor observed blue radiation from 445 to 540 nm, green radiation from 507 to 595 nm, red radiation from 632 to 697 nm, and NIR radiation from 757 to 850 nm. Each of these wavebands was observed with 4 m spatial resolution, approximately 4 times finer than the AVIRIS data. IKONOS images were georeferenced by the image provider.

IKONOS images were calibrated to percent reflectance using an empirical line method based on reflectance from the 2001 AVIRIS data. The IKONOS data were first degraded to 16 m, and two of the AVIRIS flightlines were coregistered to the degraded IKONOS data. AVIRIS spectra within the four IKONOS wavebands were averaged to generate a four-band AVIRIS image with the same spatial and spectral scale as the IKONOS data. Both data sets were sampled on a pixel-by-pixel basis to develop an empirical relationship between AVIRIS reflectances and IKONOS digital numbers. These empirical relationships were used to calibrate the IKONOS data at 4 m spatial resolution, and an IKONOS NDVI (Eq. 1) was computed. A four-endmember MESMA was conducted for the AVIRIS spectra within the IKONOS image boundaries. Pearson's correlation coefficients were calculated between each MESMA endmember and the IKONOS NDVIs aggregated from 4 m to 16 m. This procedure permitted a quantitative evaluation of MESMA results using an independent data set collected at a spatial resolution 4 times finer than the AVIRIS data.

2.7. MESMA for Degraded Images

Degradations in image spatial or spectral resolution were expected to influence MESMA results. For example, MESMA results may differ when using 15 m AVIRIS data as compared to the proposed 60 m HyspIRI data. Results could also differ if a sensor did not observe the same waveband regions as the AVIRIS sensor. To evaluate these issues, MESMA was performed using the endmember spectra (Fig. 2) to unmix spatially and spectrally degraded AVIRIS images.

2.7.1. Spatial Degradations

The effects of image spatial degradation on MESMA results were evaluated at 10 multiples of the native spatial resolutions of the 2001 and 2002 AVIRIS images over Jornada. Thus for 2001, evaluations were conducted at the following spatial resolutions: 16.6 m, 33.2 m, 49.8 m, 66.4 m, 83.0 m, 99.6 m, 116.2 m, 132.8 m, 149.4 m, and 166.0 m. Similarly for 2002, evaluations were conducted at the following spatial resolutions: 15.5 m, 31.0 m, 46.5 m, 62.0 m, 77.5 m, 93.0 m, 108.5 m, 124.0 m, 139.5 m, and 155.0 m. To generate "truth" images for comparison purposes, the MESMA results for each AVIRIS image at its native spatial resolution were also aggregated to these 10 spatial resolutions. These truth images were analyzed using the approach of Woodcock and Strahler (1987) to understand the local variance for image features at Jornada. A 3×3 filter convolution was used to calculate the local standard deviation of the MESMA results for each endmember at each spatial resolution. The convolution result was then spatially averaged within the Jornada boundary to summarize the local standard deviation at each spatial resolution. This procedure was used to summarize the loss of image spatial content at Jornada as image spatial resolution became increasingly coarse.

To assess MESMA performance at coarser spatial resolutions, the original 2001 and 2002 AVIRIS images were also degraded to each of the 10 spatial resolutions. A 4-endmember MESMA, using the endmember spectra in Fig. 2, was then conducted for each degraded image. Results for the MESMAs on the degraded AVIRIS images were compared to the degraded "truth" images from the MESMA at

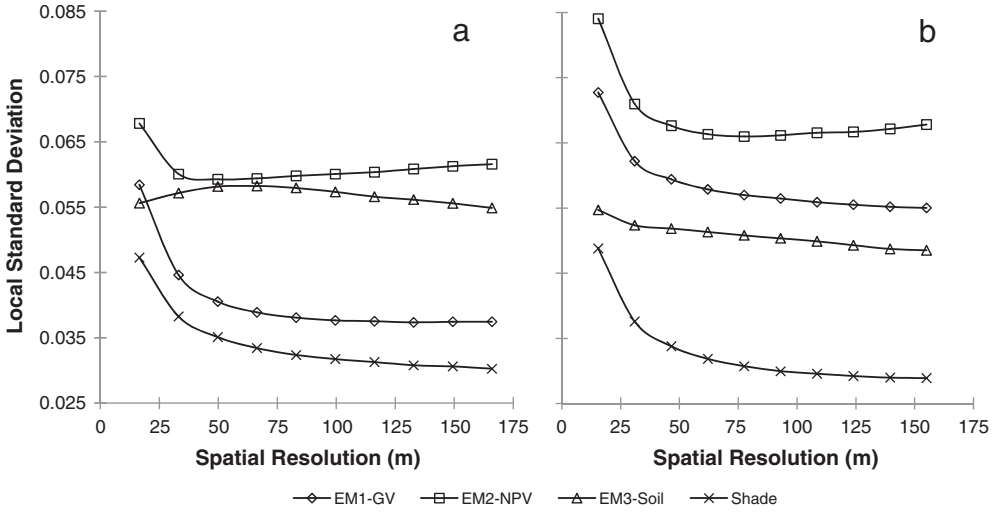

Fig. 5. Local standard deviation versus spatial resolution of MESMA endmember fractional cover estimates at Jornada on a) June 15, 2001 and b) October 9, 2002. Results were generated using the method of Woodcock and Strahler (1987) to spatially degrade the MESMA endmembers (EM) for green vegetation (GV), nonphotosynthetic vegetation (NPV), bare soil, and shade.

the native spatial resolution. Results were assessed by calculating the average bias between these images for each endmember at each spatial resolution. Also, the number of pixels with differences ranging from 0% to 1%, from 1% to 10%, and from 10% to 120% was calculated to assess the level of disagreement between images.

2.7.2. Spectral Degradations

The effects of image spectral characteristics on MESMA results were evaluated by alternatively removing the VIS/NIR, SWIR1, and SWIR2 waveband regions from the MESMA analysis. These analyses were conducted on both the 2001 and 2002 AVIRIS images at their native spatial resolutions. Six analyses were conducted, including 1) MESMA without the SWIR2 region, 2) MESMA without the SWIR1 region, 3) MESMA without the VIS/NIR region, 4) MESMA using only the SWIR2 region, 5) MESMA using only the SWIR1 region, and 6) MESMA using only the VIS/NIR region. Results for these MESMAs were compared to that from the MESMA that included all three spectral regions. Similar to the results for spatial resolution degradations, the effects of image spectral characteristics on MESMA were assessed by calculating the average bias between images and calculating the number of pixels with differences ranging from 0% to 1%, from 1% to 10%, and from 10% to 120%.

3. Results and Discussion

3.1. MESMA Results

Efforts to develop endmember spectra from the set of ground-based spectral reflectance data resulted in 30 spectra for the 2001 data set, including 6 green vegetation spectra (all mesquite), 10 nonphotosynthetic grass spectra, and 14 bare soil spectra (Fig. 2). For the 2002 data set, a total of 57 spectra were selected, including 22 green vegetation spectra, 15 nonphotosynthetic grass spectra, and 20 bare soil spectra. Of the green vegetation spectra selected in 2002, there were 8 creosote bush spectra, 7 mesquite spectra, and 7 tarbush spectra. However, as demonstrated by graphical approaches (Fig. 2b), spectral separability among the these three shrub classes could not be achieved due to similarity among the scans. Okin et al. (2001) corroborated this result, showing that MESMA was unable to reliably retrieve vegetation type in arid and semiarid environments where vegetation cover was less than 30%. In the present study, spectral separability was more evident among the spectra for green vegetation, nonphotosynthetic grass, and bare soil as compared to spectra for unique shrub species (Fig. 2).

Results of the 4-endmember MESMA for the 2001 (Fig. 3a) and 2002 (Fig. 3b) AVIRIS images were summarized using a three-band

Table 2
Average fractional cover bias between 1) endmember fractional cover from MESMAs on the spatially degraded AVIRIS images and 2) endmember fractional cover from the "truth" images, generated by spatially degrading the MESMA result at the native image spatial resolution. Results are shown for June 15, 2001 (left) and October 9, 2002 (right) image data.[a]

June 15, 2001 Images					October 9, 2002 Images				
SR	EM1	EM2	EM3	EM4	SR	EM1	EM2	EM3	EM4
(m)	GV	NPV	Soil	Shade	(m)	GV	NPV	Soil	Shade
16.6	0.0000	0.0000	−0.0000	−0.0000	15.5	0.0000	−0.0000	0.0000	−0.0000
33.2	0.0042	0.0011	−0.0022	−0.0028	31.0	0.0042	−0.0048	0.0013	−0.0006
49.8	0.0055	0.0013	−0.0030	−0.0034	46.5	0.0072	−0.0087	0.0020	−0.0005
66.4	0.0057	0.0018	−0.0035	−0.0038	62.0	0.0088	−0.0108	0.0026	−0.0006
83.0	0.0058	0.0020	−0.0035	−0.0039	77.5	0.0107	−0.0128	0.0031	−0.0010
99.6	0.0057	0.0022	−0.0035	−0.0039	93.0	0.0118	−0.0142	0.0034	−0.0010
116.2	0.0060	0.0023	−0.0035	−0.0042	108.5	0.0131	−0.0157	0.0037	−0.0011
132.8	0.0059	0.0019	−0.0033	−0.0039	124.0	0.0139	−0.0161	0.0036	−0.0014
149.4	0.0060	0.0022	−0.0034	−0.0042	139.5	0.0143	−0.0168	0.0038	−0.0014
166.0	0.0057	0.0024	−0.0032	−0.0043	155.0	0.0152	−0.0176	0.0040	−0.0016

[a] Multiple endmember spectral mixture analysis (MESMA); Spatial Resolution (SR); Endmember (EM); Green vegetation (GV); Nonphotosynthetic vegetation (NPV).

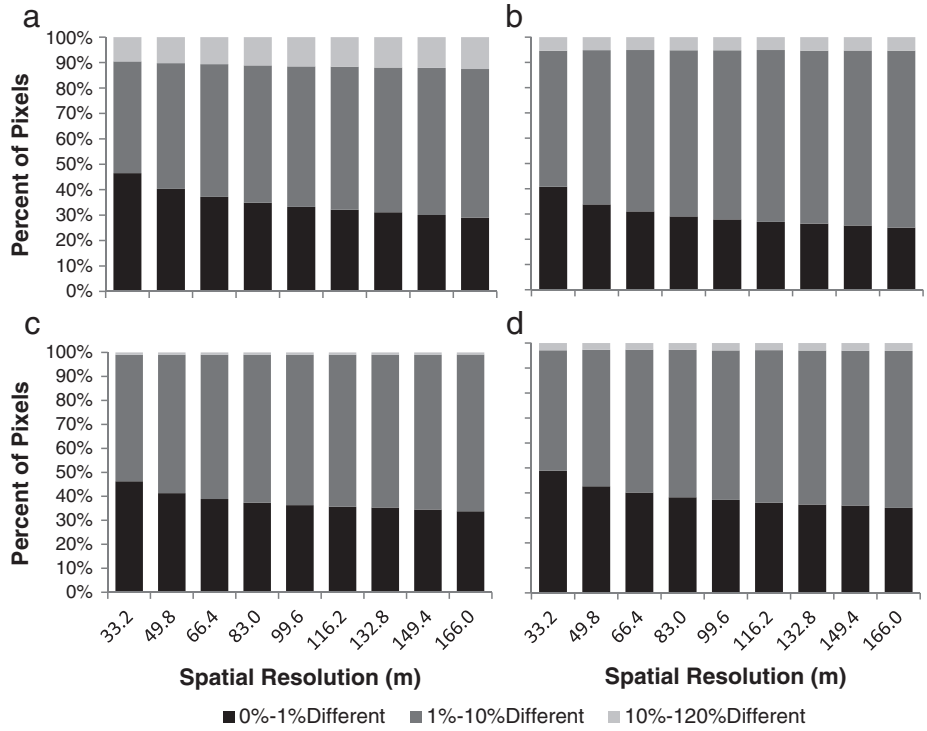

Fig. 6. Percent of image pixels that were from 0% to 1%, 1% to 10%, and 10% to 120% different when comparing 1) endmember fractional cover from multiple endmember spectral mixture analyses (MESMA) on the spatially degraded 2001 AVIRIS images and 2) endmember fractional cover from the "truth" images, generated by spatially degrading the 2001 MESMA result at the native 16.6 m image spatial resolution. Results are shown for a) green vegetation, b) nonphotosynthetic vegetation, c) bare soil, and d) shade endmembers.

RGB image where R, G, and B represented the fractional cover of nonphotosynthetic grass, green shrub vegetation, and bare soil, respectively. Subjective comparisons of the the MESMA results with the Jornada vegetation classification maps provided by Gibbens et al. (2005) demonstrated that the MESMA results were reasonable. The west central portion of Jornada was dominated by mesquite dunes in 1998 (Gibbens et al., 2005), a condition arising from gradual replacement of tobosa (*Pleuraphis mutica*) and black grama (*Bouteloua eriopoda*) grass species in the preceding century. MESMA results for AVIRIS images in 2001 and 2002 also demonstrated a dominance of green shrub vegetation in this area. An area that was transitioning from grass species to mesquite lay along the southwestern border of Jornada. Both MESMA results showed a dominance of nonphotosynthetic grass in this area with encroaching green shrub vegetation. Patches of grass dominated areas from the northwestern corner of Jornada through the center were evident in both the MESMA results and the classification map of Gibbens et al. (2005). The northern and northeastern portions of Jornada were dominated by mesquite sand hills in 1998 (Gibbens et al., 2005). MESMA results for AVIRIS images collected in 2001 and 2002 also showed a dominance of green shrub vegetation in this area.

Visual comparisons of the patterns in MESMA results demonstrated some similarities between 2001 and 2002 (Fig. 3). Sampling these two MESMA images for quantitative comparisons showed that the endmembers for green shrub vegetation, nonphotosynthetic grass vegetation, bare soil, and shade were similar, with Pearson's correlation coefficients of 0.41, 0.66, 0.67, 0.39 and average fractional cover biases of −0.08, 0.10, 0.11, and −0.13, respectively (Table 1). Spearman's correlation coefficients (not shown) were not substantially different from Pearson's correlation coefficients. Positive correlations were found for all endmembers between the two years, and relatively high correlations were found for nonphotosynthetic vegetation and bare soil endmembers. Positive biases for nonphotosynthetic vegetation and bare soil endmembers with the negative bias for green vegetation showed that lower green vegetation cover was quantified in the 2001

Table 3
Average fractional cover bias between 1) endmember fractional cover from MESMAs on the AVIRIS images with key spectral wavebands excluded and 2) endmember fractional cover from the "truth" images, which were the MESMA results using full spectrum data. Results are shown for June 15, 2001 (left) and October 9, 2002 (right) image data.[a]

	June 15, 2001 images				October 9, 2002 images			
	EM1	EM2	EM3	EM4	EM1	EM2	EM3	EM4
	GV	NPV	Soil	Shade	GV	NPV	Soil	Shade
No SWIR2	−0.0882	0.0813	0.0114	−0.0041	−0.0156	−0.0177	0.0285	0.0049
No SWIR1	−0.0215	0.0810	−0.0363	−0.0234	−0.0729	−0.0730	0.0395	0.1062
No VIS/NIR	0.1814	−0.2026	0.0262	−0.0045	0.0092	0.0702	−0.0869	0.0075
Only SWIR2	0.5623	−0.2021	−0.1036	−0.4490	0.7197	−0.1486	−0.1361	−0.4350
Only SWIR1	0.1045	−0.1204	−0.0147	0.0313	0.4387	−0.1819	−0.0394	−0.2175
Only VIS/NIR	−0.1278	0.1652	−0.0334	−0.0234	−0.1204	−0.1314	0.0688	0.1829

[a] Multiple endmember spectral mixture analysis (MESMA); Endmember (EM); Green vegetation (GV); Nonphotosynthetic vegetation (NPV); Shortwave Infrared (SWIR); Visible/Near-infrared (VIS/NIR).

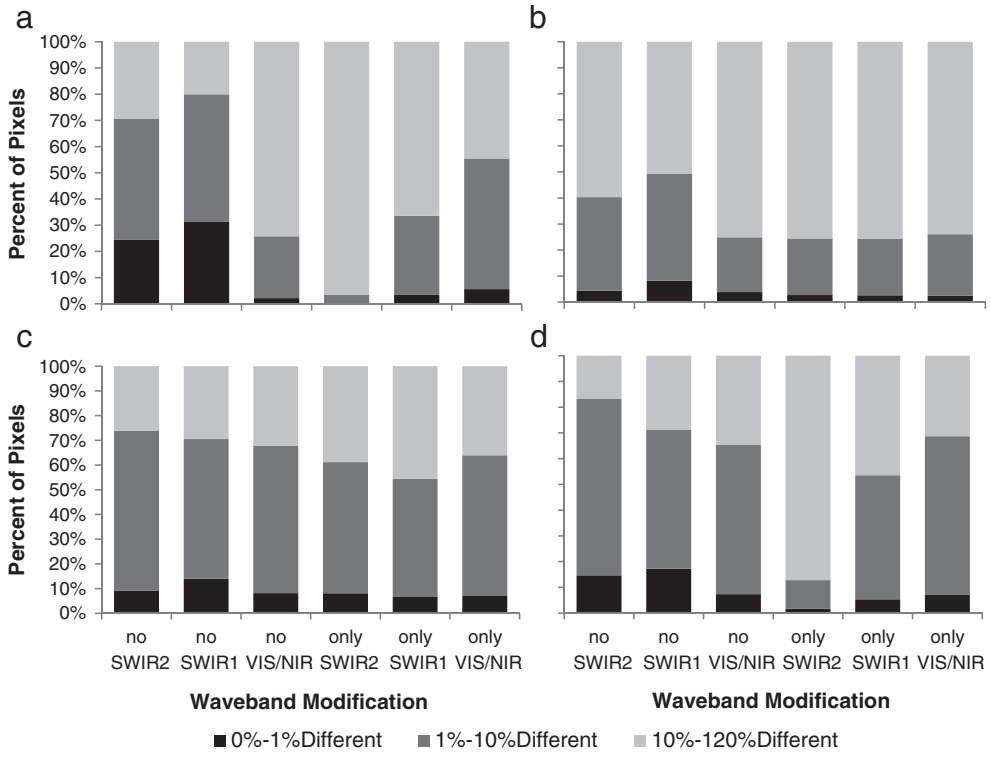

Fig. 7. Percent of image pixels that were from 0% to 1%, 1% to 10%, and 10% to 120% different when comparing 1) endmember fractional cover from multiple endmember spectral mixture analyses (MESMA) on the 2001 AVIRIS image with key spectral wavebands excluded and 2) endmember fractional cover from the "truth" image, which was the 2001 MESMA result using full spectrum data. Results are shown for a) green vegetation, b) nonphotosynthetic vegetation, c) bare soil, and d) shade endmembers.

MESMA as compared to the 2002 MESMA. Weather records at Jornada reported 15 mm and 125 mm of rainfall in the three-month period preceding the 2001 and 2002 AVIRIS overflights, respectively. Thus, higher green vegetation cover in October 2002 was likely the result of soil water recharge from the summer monsoon. Despite this important physical explanation, differences may have also resulted from errors in the atmospheric correction of the two AVIRIS images and from differences in MESMA calculations due to the use of independent ground-based spectral data sets. Also, since the shade endmember showed the greatest absolute fractional cover bias (0.13) and the lowest correlation coefficient (0.39) between the two years, the modeled differences in shade fractional cover likely affected the cover fractions for the other endmembers. These considerations highlight a need for caution in the use of MESMA results. Due to the sensitivity of MESMA results to shade assumptions and spectral characteristics of the images and endmember spectra, the technique may be most useful for relative comparisons of fractional cover rather than absolute fractional cover estimates.

With correlation coefficients of 0.73 and 0.58 in 2001 and 2002, respectively, the NDVI from AVIRIS data was well correlated with the green vegetation endmember from MESMAs on the AVIRIS data (Table 1). These correlations were positive as expected, because the NDVI is sensitive to green biomass. Correlations between the CAI and the green vegetation endmember were much weaker compared to that for NDVI. The nonphotosynthetic grass endmember was positively correlated with the CAI with correlation coefficients of 0.56 and 0.40 in 2001 and 2002, respectively. This agreement highlighted the sensitivity of the CAI to cellulose in the nonphotosynthetic grass species at Jornada and demonstrated that MESMA was reasonably able to map this vegetation characteristic. The CAI also exhibited strong negative correlations with the bare soil endmember in both years. As cellulose increased with increasing vegetation cover, bare soil cover was expected to decrease, resulting in the negative correlations. Summing the cover fraction for the green vegetation and nonphotosynthetic vegetation endmembers and correlating to CAI, the correlation coefficients were 0.59 and 0.60 in 2001 and 2002, respectively. These correlations were greater than that between CAI and nonphotosynthetic vegetation alone. Thus, CAI was sensitive to the combined effect of green and nonphotosynthetic vegetation cover. The NDVI was not sensitive to this combination. These correlations between the MESMA endmembers and spectral indices help to justify the MESMA results by demonstrating expected relationships.

With correlation coefficients of 0.71 and 0.57 for northwestern and southwestern subsets of Jornada, respectively, NDVI from independent IKONOS images was well correlated with the green vegetation endmember from MESMAs on the 2001 AVIRIS data (Table 1). This means the fractional green vegetation cover provided by MESMA was comparable to that estimated using a common vegetation index with multispectral imagery. An advantage of MESMA using AVIRIS spectra was that it provided additional fractional cover information for other endmembers, which was not easily estimated using multispectral data. For example, with correlation coefficients lower than 0.41, fractional cover estimates for bare soil and for the sum of green and nonphotosynthetic vegetation were not very well correlated with IKONOS NDVI data. Fractional cover estimates for nonphotosynthetic vegetation were negatively correlated with NDVI for both IKONOS images, a reasonable result considering that nonphotosynthetic grass vegetation was likely inversely proportional with encroaching green shrub vegetation across Jornada.

From the 2002 MESMA where endmember spectra were available for three shrub species, 20%, 74%, and 6% of image pixels were classified using creosote bush, mesquite, and tarbush endmember spectra, respectively. This result was favorable, because mesquite was likely the most dominate shrub across the range, while creosote bush and tarbush were less common (Gibbens et al., 2005). Spatial patterns of the classification result for these shrubs roughly followed expected

results with mesquite more common in western and northeastern areas, creosote bush more common in the northern and eastern regions, and tarbush more common in the southeast (Fig. 4). However, the spatial patterns are also somewhat random due to the difficulty in achieving spectral separability among the endmember spectra for the shrub species (Fig. 2b). Also, because the vegetation classification map in Fig. 4 focused only on the MESMA result for the green vegetation endmember, the result was probably most reliable for the pixels in which the green vegetation endmember was most dominant. Fractional cover for the green vegetation endmember was dominant (greater than fractional cover for the nonphotosynthetic vegetation and bare soil endmembers) for only 18% of the image pixels, and 14% of the image pixels were dominated by mesquite. By contrast, fractional cover for the bare soil endmember was dominate for 48% of the image pixels. Plentiful bare soil and relatively low creosote bush and tarbush coverage likely contributed to the difficulty in distinguishing between shrub species at Jornada. Spectral measurements of shaded lower leaves within a shrub canopy may have helped identify unique shrub species, since transmission and reflectance within the canopy is expected to depend on plant morphology (Fitzgerald et al., 2005).

3.2. Spatial Scale Effects

With a few exceptions, the local standard deviation of image features at Jornada tended to decrease as the MESMA result at the native image spatial resolution was spatially degraded (Fig. 5). In particular, the greatest loss of spatial detail occurred from the native resolution of the AVIRIS images (~15 m) to around 50 m. This result highlighted an important difference between the data collected by AVIRIS and the 60 m data expected from the HyspIRI sensor. For Jornada, 60 m resolution data does not substantially increase land cover information content compared to 150 m data. In fact, even the 15 m airborne AVIRIS images did not adequately resolve the spatial features at Jornada, since a peak in local standard deviation should be found at the optimum spatial resolution (Woodcock and Strahler, 1987). This result demonstrated that the optimum spatial resolution for resolving spatial features at Jornada is less than 15 m, a result supported by Pelgrum et al. (2000).

The average bias between endmember fractional cover from MESMAs on the degraded AVIRIS images and that from the "truth" images was not more than 0.006 and 0.02 for the 2001 and 2002 data, respectively (Table 2). Biases were small, indicating that MESMA results for spatially degraded AVIRIS images were comparable to spatial aggregations of the MESMA results for images at finer spatial scales. This means that coarser image resolution did not grossly effect MESMA performance. Rather, it only affected the spatial detail with which MESMA was able to resolve endmember fractional cover. In comparing the 2001 MESMAs for spatially degraded images with the "truth" images, over 90% of image pixels had endmember fractional cover values that were less than 10% different (Fig. 6). At a spatial resolution of 33.2 m, around 45% of pixels had endmember fractional cover values less than 1% different. The percentage of pixels less than 1% different decreased to around 30% as the image spatial resolution increased to 166.0 m. These results were consistent among all four endmembers. Similar patterns were observed in comparing the 2002 MESMAs for spatially degraded images with the 2002 "truth" images (not shown).

3.3. Spectral Waveband Effects

The average bias between endmember fractional cover from MESMAs on the AVIRIS images with key wavebands excluded were variable depending on the test case (Table 3). Average biases for MESMAs based on spectrally degraded images were often greater than that for spatially degraded images by a factor of 10 or 100 (Tables 2 and 3). Therefore, MESMA results were much more sensitive to the spectral wavebands used in the analysis than to the spatial resolution of the images. Greater average biases were typically found for the cases excluding VIS/NIR wavebands, including only SWIR2 wavebands, and including only SWIR1 wavebands (Table 3). This result highlighted the importance of the VIS/NIR wavebands in guiding the MESMA toward reasonable results for this semiarid rangeland application. Substantially larger biases were typically found for MESMAs based solely on reflectance in the SWIR2 region from 2330 to 2339 nm. Only for the nonphotosynthetic vegetation did MESMA results for this test case compare well with other test cases, likely due to the sensitivity of the SWIR2 wavebands to the cellulose in grass vegetation (Nagler et al., 2003). With average biases of 0.5623 and 0.7197 in 2001 and 2002, respectively, the SWIR2 bands alone did not provide an effective way to quantify green vegetation. However, the SWIR2 and SWIR1 regions were more effective at quantifying green vegetation when used in combination with VIS/NIR, as compared to any of the three waveband regions alone.

Similar conclusions can be drawn from the percentage of pixels that were from 0% to 1%, 1% to 10%, and 10% to 120% different when comparing endmember fractional cover for MESMAs with spectral wavebands excluded with the "truth" MESMA based on full spectrum data for 2001 (Fig. 7). Results for 2002 (not shown) were similar. Agreement for the green vegetation endmember was poor when the VIS/NIR region was removed from the analysis. The best agreement for green vegetation was found when using a combination of VIS/NIR and SWIR wavebands to conduct MESMA analyses. Again, the higher sensitivity of MESMA to adjustments in spectral characteristics (Fig. 7) as opposed to spatial resolution characteristics (Fig. 6) was found.

4. Conclusions

Multiple endmember spectral mixture analysis (MESMA) was an effective image processing approach for using hyperspectral remote sensing data to map green vegetation, nonphotosynthetic vegetation, and bare soil on a semiarid rangeland: the Jornada Experimental Range in southwestern New Mexico. However, MESMA results were sensitive to the characteristics of the image spectra and endmember spectra used in the analysis. MESMA results were substantially less sensitive to the spatial resolution of the input images. Thus, MESMA is a valuable data analysis tool for airborne and satellite-based imaging spectroscopy applications that lack optimum image spatial resolution to resolve the spatial features present in the scene. Neither AVIRIS nor the proposed HyspIRI sensor offer adequate image spatial resolution to resolve spatial features at Jornada. However, spatial resolution is secondary in importance to spectral resolution for MESMA. Distinguishing between different shrub species at Jornada was not supported using MESMA with the available endmember spectra. While MESMA techniques did distinguish between green shrub vegetation and nonphotosynthetic grass vegetation, the techniques could not distinguish the three primary shrub species: mesquite, creosote bush, and tarbush. Selection of the spectral wavebands that offered the best information for MESMA was subjective and not straightforward. Extensive understanding of and experience with the input data sets is required to obtain reliable MESMA results. Future work will focus on the development of techniques to objectively select wavebands for inclusion in the MESMA analysis.

Acknowledgements

This research was partially conducted with funds from the NASA Headquarters, Science Mission Directorate, Research Opportunities in Space and Earth Sciences (ROSES) program entitled HyspIRI Preparatory Activities Using Existing Imagery. The authors credit Dr. Jerry Ritchie (1937–2009), former Research Soil Scientist at USDA-ARS and long-term contributor at Jornada, for his efforts to collect and organize the ground-based spectral data used in this study.

References

Asner, G., & Heidebrecht, K. (2002). Spectral unmixing of vegetation, soil and dry carbon cover in arid regions: comparing multispectral and hyperspectral observations. *International Journal of Remote Sensing*, *23*(19), 3939–3958.

Asner, G., Wessman, C., Bateson, C., & Privette, J. (2000). Impact of tissue, canopy, and landscape factors on the hyperspectral reflectance variability of arid ecosystems. *Remote Sensing of Environment*, *74*(1), 69–84.

Buffington, L. C., & Herbel, C. H. (1965). Vegetational changes on a semidesert grassland range from 1858 to 1963. *Ecological Monographs*, *35*(2), 139–164.

Chehbouni, A., Goodrich, D., Moran, M., Watts, C., Kerr, Y., & Dedieu, G. (2000). A preliminary synthesis of major scientific results during the SALSA program. *Agricultural and Forest Meteorology*, *105*(1–3), 311–323.

Dennison, P., & Roberts, D. (2003). Endmember selection for multiple endmember spectral mixture analysis using endmember average RMSE. *Remote Sensing of Environment*, *87*(2–3), 123–135.

Fitzgerald, G., Pinter, P., Jr., Hunsaker, D., & Clarke, T. (2005). Multiple shadow fractions in spectral mixture analysis of a cotton canopy. *Remote Sensing of Environment*, *97*(4), 526–539.

Gibbens, R., McNeely, R., Havstad, K., Beck, R., & Nolen, B. (2005). Vegetation changes in the Jornada Basin from 1858 to 1998. *Journal of Arid Environments*, *61*(4), 651–668.

Green, R. O., Eastwood, M. L., Sarture, C. M., Chrien, T. G., Aronsson, M., Chippendale, B. J., et al. (1998). Imaging spectroscopy and the Airborne Visible/Infrared Imaging Spectrometer (AVIRIS). *Remote Sensing of Environment*, *65*(3), 227–248.

Havstad, K., Kustas, W., Rango, A., Ritchie, J., & Schmugge, T. (2000). Jornada Experimental Range: a unique arid land location for experiments to validate satellite systems. *Remote Sensing of Environment*, *74*(1), 13–25.

Hoyt, C. A. (2002). The Chihuahuan Desert: diversity at risk. *Endangered Species Bulletin*, *27*(2), 16–17.

Kotchenova, S., Vermote, E., Matarrese, R., & Klemm, F., Jr. (2006). Validation of a vector version of the 6S radiative transfer code for atmospheric correction of satellite data. Part I: Path radiance. *Applied Optics*, *45*(26), 6762–6774.

Li, L., Ustin, S., & Lay, M. (2005). Application of AVIRIS data in detection of oil-induced vegetation stress and cover change at Jornada, New Mexico. *Remote Sensing of Environment*, *94*(1), 1–16.

Mansour, K., Mutanga, O., Everson, T., & Adam, E. (2012). Discriminating indicator grass species for rangeland degradation assessment using hyperspectral data resampled to AISA Eagle resolution. *ISPRS Journal of Photogrammetry and Remote Sensing*, *70*, 56–65.

Mesinger, F., DiMego, G., Kalnay, E., Mitchell, K., Shafran, P., Ebisuzaki, W., et al. (2006). North American regional reanalysis. *Bulletin of the American Meteorological Society*, *87*(3), 343–360.

Nagler, P., Inoue, Y., Glenn, E., Russ, A., & Daughtry, C. (2003). Cellulose absorption index (CAI) to quantify mixed soil-plant litter scenes. *Remote Sensing of Environment*, *87*(2–3), 310–325.

Okin, G., Roberts, D., Murray, B., & Okin, W. (2001). Practical limits on hyperspectral vegetation discrimination in arid and semiarid environments. *Remote Sensing of Environment*, *77*(2), 212–225.

Pelgrum, H., Schmugge, T., Rango, A., Ritchie, J., & Kustas, B. (2000). Length-scale analysis of surface albedo, temperature, and normalized difference vegetation index in desert grassland. *Water Resources Research*, *36*(7), 1757–1765.

Privette, J., Asner, G., Conel, J., Huemmrich, K., Olson, R., Rango, A., et al. (2000). The EOS Prototype Validation Exercise (PROVE) at Jornada: overview and lessons learned. *Remote Sensing of Environment*, *74*(1), 1–12.

Rango, A., Huenneke, L., Buonopane, M., Herrick, J., & Havstad, K. (2005). Using historic data to assess effectiveness of shrub removal in southern New Mexico. *Journal of Arid Environments*, *62*(1), 75–91.

Reda, I., & Andreas, A. (2004). Solar position algorithm for solar radiation applications. *Solar Energy*, *76*(5), 577–589.

Roberts, D., Gardner, M., Church, R., Ustin, S., Scheer, G., & Green, R. (1998). Mapping chaparral in the Santa Monica Mountains using multiple endmember spectral mixture models. *Remote Sensing of Environment*, *65*(3), 267–279.

Rouse, J. W., Jr., Haas, R. H., Schell, J. A., & Deering, D. W. (1973). Monitoring the vernal advancement and retrogradation (green wave effect) of natural vegetation. *Program Report RSC 1978–1. Tech. rep.* College Station: Remote Sensing Center, Texas A&M University (93 pp. NTIS no. E73-10693).

Thenkabail, P. S., Smith, R. B., & DePauw, E. (2000). Hyperspectral vegetation indices and their relationships with agricultural crop characteristics. *Remote Sensing of Environment*, *71*(2), 158–182.

Woodcock, C., & Strahler, A. (1987). The factor of scale in remote sensing. *Remote Sensing of Environment*, *21*(3), 311–332.

Yang, C., Everitt, J., & Johnson, H. (2009). Applying image transformation and classification techniques to airborne hyperspectral imagery for mapping Ashe juniper infestations. *International Journal of Remote Sensing*, *30*(11), 2741–2758.